Journal of the American Chemical Society 139.29 (2017): 10079-10086
DOI: https://doi.org/10.1021/jacs.7b05182

Supporting Information

Ionic Conductivity and Potential Application for Fuel Cell of a Modified Imine-based Covalent Organic Framework

Carmen Montoro,[†] David Rodríguez-San-Miguel,[†] Eduardo Polo,[†] Ricardo Escudero-Cid,[‡] Maria Luisa Ruiz-González,[£] Jorge A. R. Navarro,[§] Pilar Ocón[*‡] and Félix Zamora[*†,ǁ]

[†] Departamento de Química Inorgánica, Institute for Advanced Research in Chemical Sciences (IAdChem) and Condensed Matter Physics Center (IFIMAC). Universidad Autónoma de Madrid. 28049 Madrid, Spain.

[‡] Departamento de Química Física Aplicada. Universidad Autónoma de Madrid. 28049 Madrid, Spain.

[£] Departamento de Química Inorgánica, Universidad Complutense de Madrid, 28040 Madrid, Spain.

[§] Departamento de Química Inorgánica. Universidad de Granada. 18071 Granada, Spain.

[ǁ] Instituto Madrileño de Estudios Avanzados en Nanociencia (IMDEA-Nanociencia), Cantoblanco, Madrid E-28049, Spain.

Table of Contents

I. General Methods

II. Synthesis of the materials

III. ATR-FT-IR Spectra

IV. Powder X-Ray Diffraction

V. Chemical Stability Test

VI. Solid-State Nuclear Magnetic Resonance Spectroscopy

VII. Thermogravimetric Analysis

VIII. N_2 Adsorption Isotherms

IX. X-Ray Photoelectron Spectroscopy

X. Transmission Electron Microscopy

XI. Scanning Electron Microscopy

XII. Film Characterization

XIII. Conductivity measurements

XIV. Fuel Cell measurements

XV. References

I. General Methods

All general reagents and solvents were commercially available and used as received except 1,3,5-tris-(4-aminophenyl)benzene (TAPB) that was prepared following the procedure described in reference [1].

Elemental Analysis (EA) were obtained using LECO CHNS-932 elemental analyser.

Thermogravimetric analysis (TGA) of samples were run on a Thermobalance TGA Q-500 thermal gravimetric analyser of TA Instruments. The sample was deposited in a platinum pan. N_2 was used as a purge gas at a flow of 90 mL min^{-1}. The samples were heated at 10 K min^{-1} from room temperature to 1173 K.

ATR-FT-IR spectroscopy was recorded in a Perkin Elmer Spectrum 100 with a PIKE Technologies MIRacle Single Reflection Horizontal ATR Accesory with a spectral range of 4000-650 cm^{-1}.

Powder X-Ray Diffraction (PXRD) patterns were obtained on a PANalytical´s X'Pert PRO diffractometer using CuKα radiation (λ = 1.5406 Å) by means of a scan in the 5-90° 2Θ range with 0.05° steps. The compounds were manually grounded in an agate mortar and then deposited in the hollow of a zero-background silicon sample holder.

The X-ray diffraction patterns of pressed pellets and films were acquired on a single crystal Bruker D8 Venture diffractometer using CuKα radiation (λ = 1.5406 Å) under transmission and reflection modes using a single crystal Bruker D8 Venture instrument.

Static solid-state (ss) and pulse field gradient (PFG) nuclear magnetic resonance (NMR) measurements were carried out at room temperature on a Bruker Avance III 400 MHz WB solid state spectrometer with a triple probe channel of 4mm, rotors of ZrO and a stopper of Kel-F. The spectra were acquired at a resonance frequency of 400.13 MHz for ^{1}H and 155.50 MHz for ^{7}Li without sample spinning. ^{1}H spectra were measured with direct radiation, a spectral width of 200 kHz, relaxation time of 5 s and pulses of π/2 at 90 kHz. ^{7}Li spectra were measured with direct radiation, a spectral width of 200 kHz, relaxation time of 4 s and pulses of π/9 at 25 kHz. ^{1}H was referred to H_2O as a secondary reference, to 4.77 ppm relative to TMS as a primary reference. ^{7}Li chemical shift is referenced to the external standard references of 0.1M LiCl in D_2O as primary reference. The samples were measured at two different relative humidity

conditions, 22 % and 100 %. For the last case, the samples were placed in a chamber saturated with water vapor and were kept there for 48 h in case of the sample with Li and 5 days for the rest to ensure the establishment of equilibrium state.

The PFG NMR spectroscopy was performed on a 9.4 T Bruker solid-state NMR instrument with an AVANCE 400 MHz spectrometer equipped with a Diff 60 PFG probe. Recycle delay used was 5s for both nuclei. During the stimulated spin echo pulse sequence the maximum gradient field used was 1250 G cm^{-1}. The spin-echo intensity was determined by the expression $I/I_0= \exp (-D (2\pi\gamma G_i\delta)^2(\Delta-\delta/3)1x10^4)$.

Solid-State MAS NMR Spectra were obtained in a Bruker AVANCE-400 spectrometer. ^{13}C CP-MAS NMR spectra were carried out using a standard cross-polarization pulse sequence. The samples were spin at 10 kHz. Spectrometer frequency was set to 100.62 MHz. A contact time of 2 ms and a period between successive accumulations of 5 s were used. The number of scans was 600. Chemical shift values were referenced to TMS. For ^7Li MAS NMR spectra, the external magnetic field used was 9.4 T and the resonance frequency was 155.50 MHz. The experiments were performed at room temperature by rotating the sample around the magic angle (54º44 ', with respect to the external magnetic field) with a speed of 10 kHz. For the acquisition of the spectra single pulse sequences were used, with the following parameters: irradiation pulse duration of 3.5 μs; Time interval between successive accumulations of 5s; Number of accumulations of 160. To determine the chemical shift values in the spectra, a 1M LiCl solution was used as a reference.

N_2 and H_2O vapour adsorption isotherms were measured at 77 K on a Micromeritics Tristar 3000 volumetric instrument and at 298 K on a volumetric apparatus Quantachrome Hydrosorb 1000 HT where temperature was controlled by a Julabo thermostatic bath, respectively. Prior to measurements, powder samples were heated 7 h at 423 K and outgassed to 10^{-6} Torr.

Atomic Force Microscope (AFM) measurements were made in dynamic mode using a Nanotec Electronica System operating at room temperature in ambient air conditions. The images were processed using WSxM (freely downloadable scanning probe microscopy software from www.nanotec.es). For AFM measurements, commercial Olympus Si/N cantilevers were used with a nominal force constant of 0.75 N/m.

Field Emission Scanning Electron Microscopy (FESEM) studies were performed on a Philips XL 30 S-FEG microscope. Samples were previously coated with chromium in a sputter Quorum Q150T-S.

Scanning Electron Microscopy (SEM) images were taken in a JEOL JM6400 equipped with a 40 kV microprobe.

X-ray photoelectron spectroscopy (XPS) spectra were recorded on a Kratos AXIS Ultra DLD spectrometer using a monochromatic Al Kα irradiation source (1486.6 eV) operated at 600 W.

Transmission Electron Microscopy (TEM). High Resolution Transmission Electron Microscopy (HRTEM) images were obtained in a *JEOL-JEM GRAND ARM 300cF* microscope equipped with a Cs Corrector (ETA-JEOL). A precise measurement of the aberrations and an optimized correction has been done using the corrector control software JEOL COSMO. The accelerating voltage was set to 60 kV in order to minimize the sample damage. The HRTEM images were acquired by a slow-scan CCD camera (4096 x 4096 pixels, Gatan OneView Camera). *Sample preparation*: 1 mg of **RT-COF-1AcB** was sonicated in 3 mL of isopropanol: water 8:2 at 320 W and 37 kHz in a sonication bath (Elma Sonic P300H) for 30 minutes. The resulting suspension centrifuged at 1500 rpm (211 rcf) for 5 minutes. Several drops of the suspension were casted on the TEM grids (200 mesh, copper-based holey carbon film, EMS).

II. Synthesis of the materials

The synthesis and characterization of **RT-COF-1** and **RT-COF-1Ac** were made according to the published procedures described previously by us.[1,2]

RT-COF-1AcB. 100 mg (0.285 mmol) of 1,3,5-tris(4-aminophenyl)benzene (TAPB) were dissolved in 14.2 mL of glacial acetic acid. 46 mg (0.285 mmol) of 1,3,5-benzenetricarbaldehyde (BTCA) were dissolved in 14.2 mL of glacial acetic acid. Both solutions were mixed at room temperature and an orange gel formed immediately. After 72 h, the gel was washed with tetrahydrofuran (100 mL) and isolated by filtration. The resulting solid was dried under open atmosphere over 2 days to yield 163 mg (86 % yield) of **RT-COF-1AcB** as a red solid.

Elemental analysis calculated for $(C_{33}H_{21}N_3)(CH_3COOH)_{3.5}$ (**RT-COF-1AcB**): C: 71.75 %, H: 5.23 %, N: 6.28 %, volatile 31 %; Found: C 68.78 %, H: 5.50 %, N: 6.44 %, volatile: 27 %.

LiCl@RT-COF-1. 100 mg (0.285 mmol) of 1,3,5-tris(4-aminophenyl)benzene (TAPB) were dissolved in 5 mL of m-cresol and 46 mg (0.285 mmol) of 1,3,5-benzenetricarbaldehyde (BTCA) were dissolved in another 5 mL of the same solvent and 1 mL of glacial acetic acid. Both solutions were mixed at room temperature and a yellow gel formed immediately. After 30 minutes of reaction, the gel was suspended in 100 mL of 30 g/L LiCl aqueous solution and the mixture was stirred during 24 h. Then, it was filtered and dried at 373 K under vacuum (50 mbar) overnight to yield 155 mg (88 % yield) of **LiCl@RT-COF-1** as a brown solid.

Elemental analysis calculated for $(C_{33}H_{21}N_3)(LiCl)_{1.3}(H_2O)_{4.5}(C_7H_8O)_{0.2}$ (**LiCl@RT-COF-1**): C, 66.93 %; H, 5.16 %; N, 6.81 %; Found: C, 66.95 %; H, 5.65 %; N, 6.80 %. XPS analysis estimate the presence of Cl into the cavities in a Cl:N 1:4 ratio.

The purity of the synthesized systems was checked by PXRD, EA, TGA, ICP-MS and N_2 adsorption isotherm measurements.

Pellets and Films Fabrication

Pellets of RT-COF-1 *and* ***LiCl@RT-COF-1*****.** They were prepared submitting around 50 mg of the powder material upon a pressure of 400 MPa, using a uniaxial hydraulic press, for 5 min. SEM image of **LiCl@RT-COF-1** pellet is shown in Figure S17.

RT-COF-1Ac** and **RT-COF-1AcB films. They were prepared submitting around 30 mg of the powder material upon a pressure of 400 MPa, using a uniaxial hydraulic press, for 5 min.

LiCl@RT-COF-1 film. 20 µL of acetic acid were added to 40 mg of **LiCl@RT-COF1** and mixed softly using an agate mortar. After approximately 2 minutes, when it is observed that the powder is dry, a pressure of 400 MPa is applied using a uniaxial hydraulic press, for 5 min. The spectroscopic characterization of **LiCl@RT-COF-1** film matches that of the starting material, meaning there is no incorporation of acetic acid inside the structure of the COF.

All films present dimensions of 13 mm of diameter and a thickness of 0.01-0.03 cm. These conformations do not affect the crystallinity of the materials showing all of them a good mechanical strength.

III. ATR-FT-IR Spectra

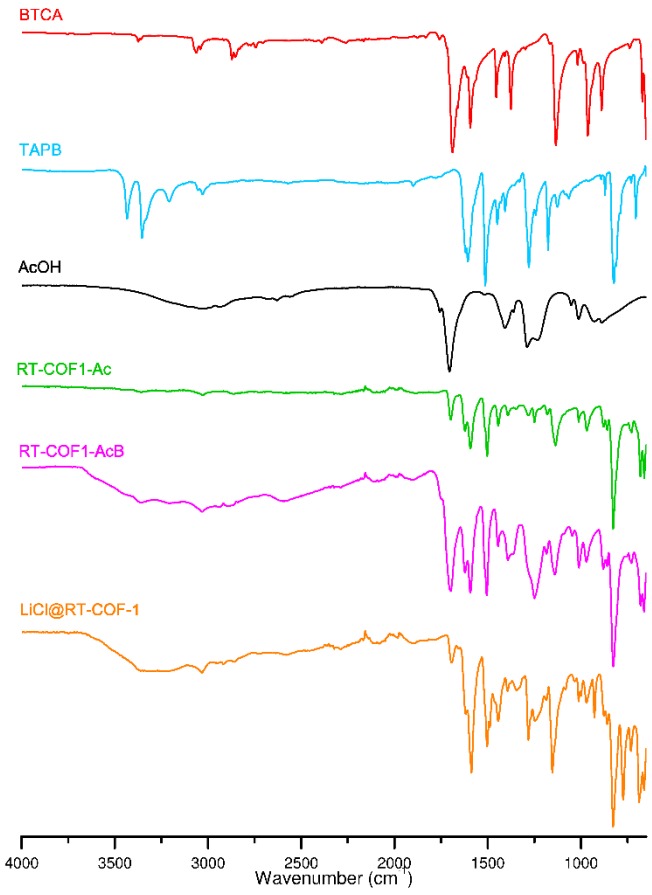

Figure S1. ATR-FT-IR spectra of monomers BTCA and TAPB, acetic acid, **RT-COF-1Ac**, **RT-COF-1AcB** and **LiCl@RT-COF-1**.

IV. Powder X-Ray Diffraction

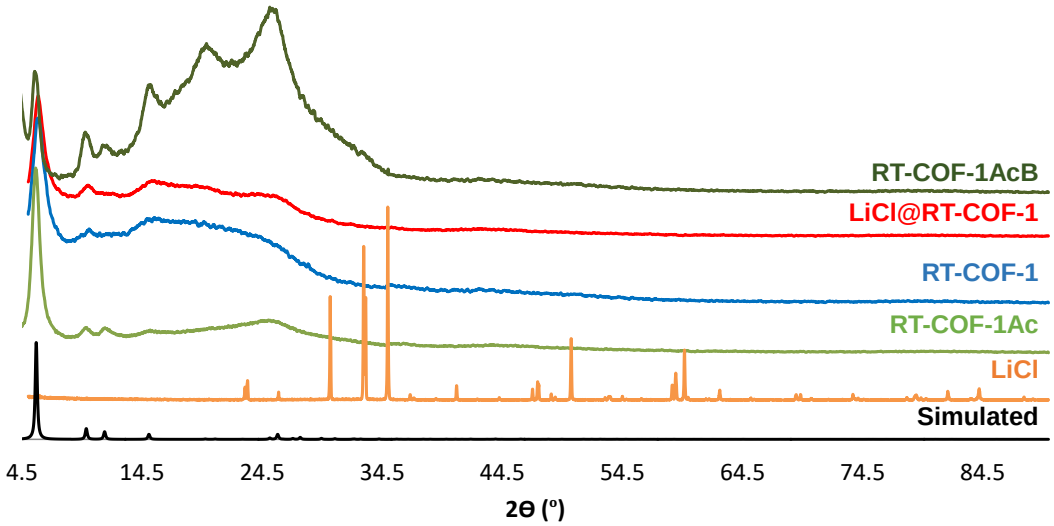

Figure S2. PXRD patterns for **LiCl@RT-COF-1**, **RT-COF-1**, **RT-COF-1Ac**, **RT-COF-1AcB**, pure LiCl and simulated pattern of **RT-COF-1**.

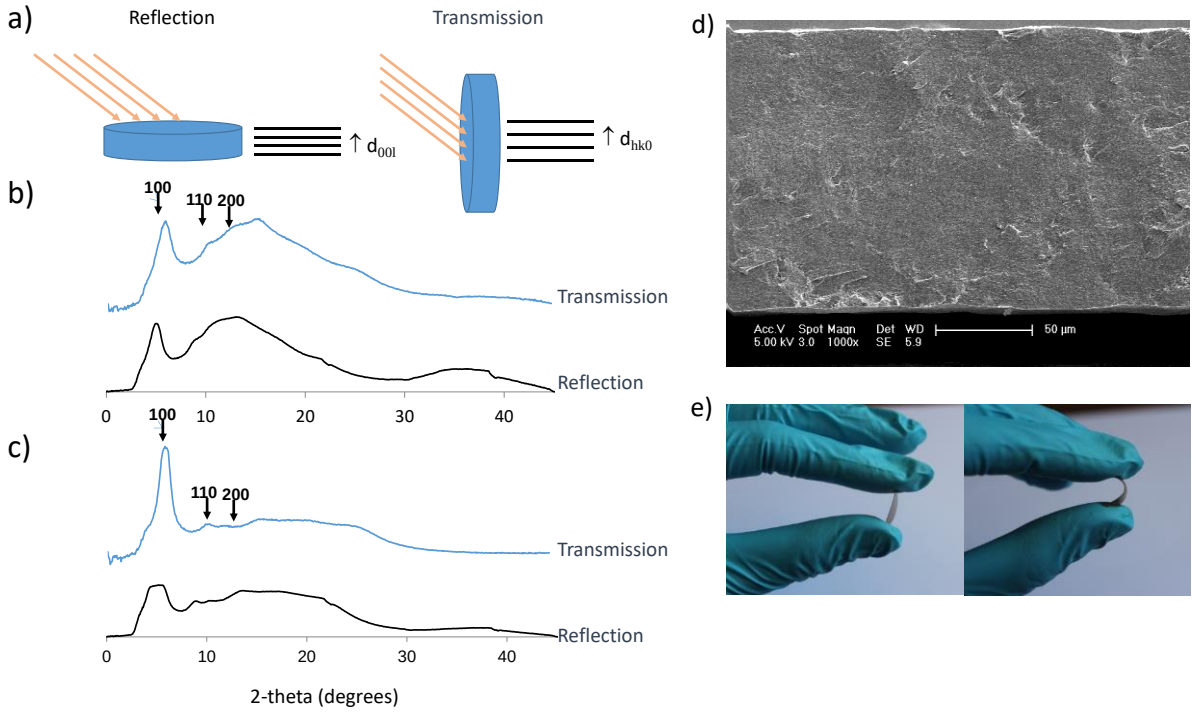

Figure S3. a) Scheme of the orientations parallel (reflection) and perpendicular (transmission) of the measurements carried out in both the **RT-COF-1Ac** pellet and the film. b) Diffractograms of **RT-COF-1Ac** in a pellet prepared applying a pressure of 15 MPa, and c) in a thin film prepared applying a pressure of 300 MPa. d) SEM micrograph of the **RT-COF-1Ac** film. e) Pictures of the **RT-COF-1Ac** film showing its flexibility.

V. Chemical stability tests

Stability tests were carried out by immersing 10 mg of **RT-COF-1Ac** in 1 mL of aqueous solutions of HCl (12 M) or NaOH (14 M) and stirring the suspension for 72 hours. Then, the samples were washed with water and dried under vacuum at 423 K for 24 hours. In the case of the acidic treatment, 86 % of the solid material is recovered, and with the basic treatment, 90 %. These values are similar to those reported for other imine-based COFs.[3] Moreover, there is no significant loss of crystallinity, as can be observed in the PXRD patterns.

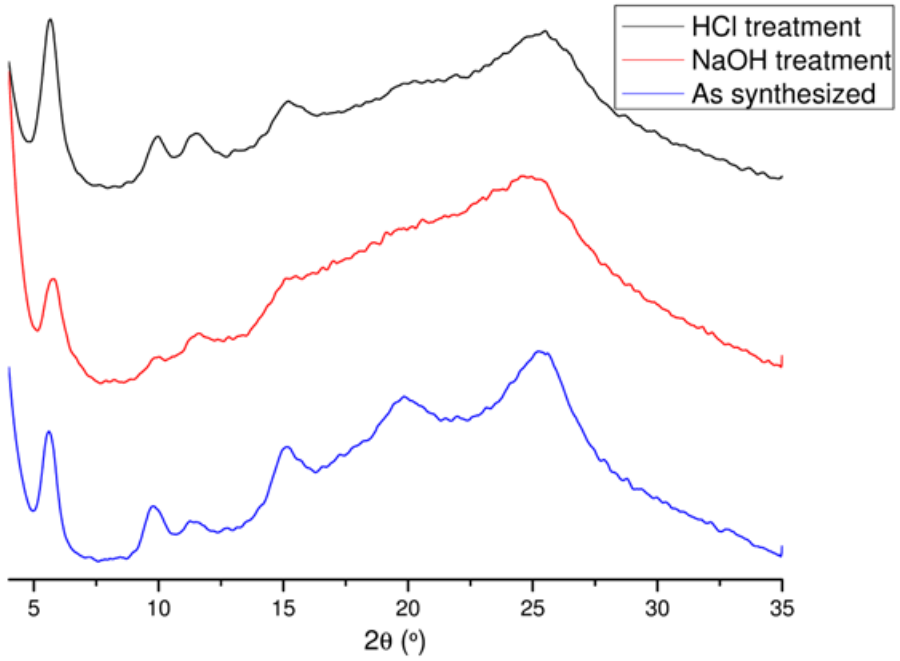

Figure S4. PXRD patterns of **RT-COF-1Ac** before (blue), and after treatment with NaOH 14 M (red) and HCl 12 M (black).

VI. Solid-State Nuclear Magnetic Resonance Spectroscopy

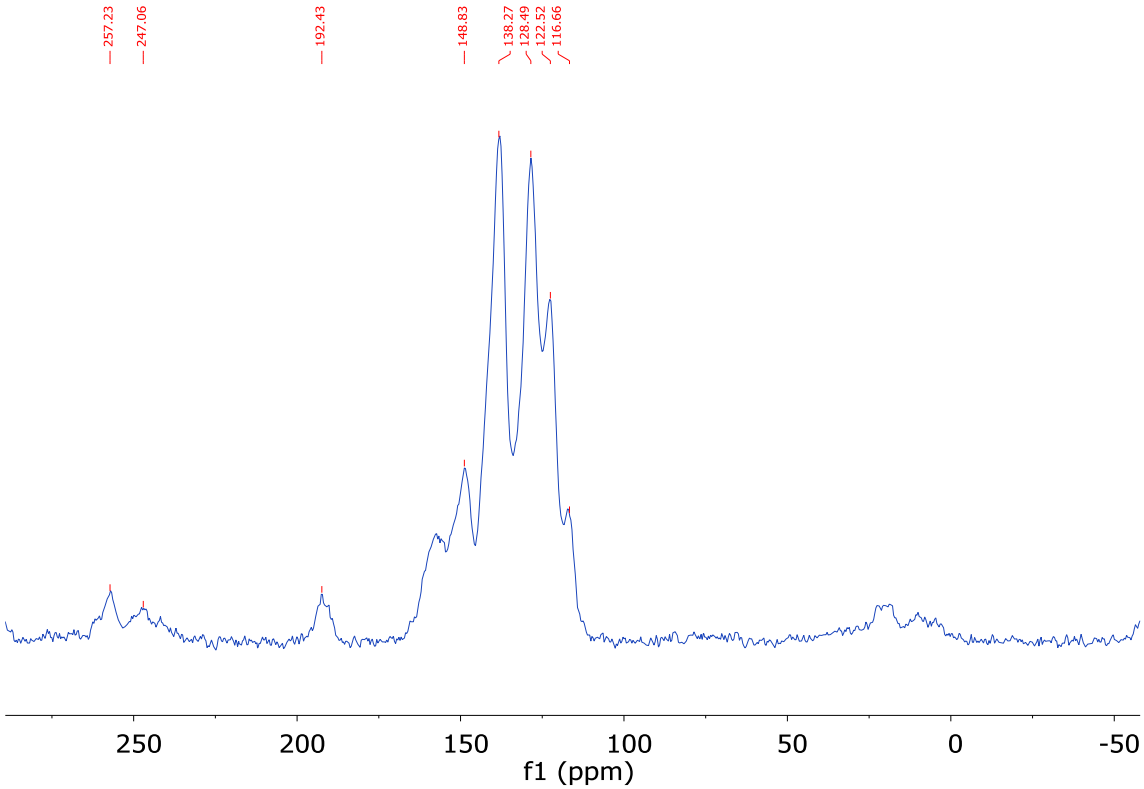

Figure S5. Solid-state ^{13}C CP-MAS NMR spectra of **RT-COF-1.**

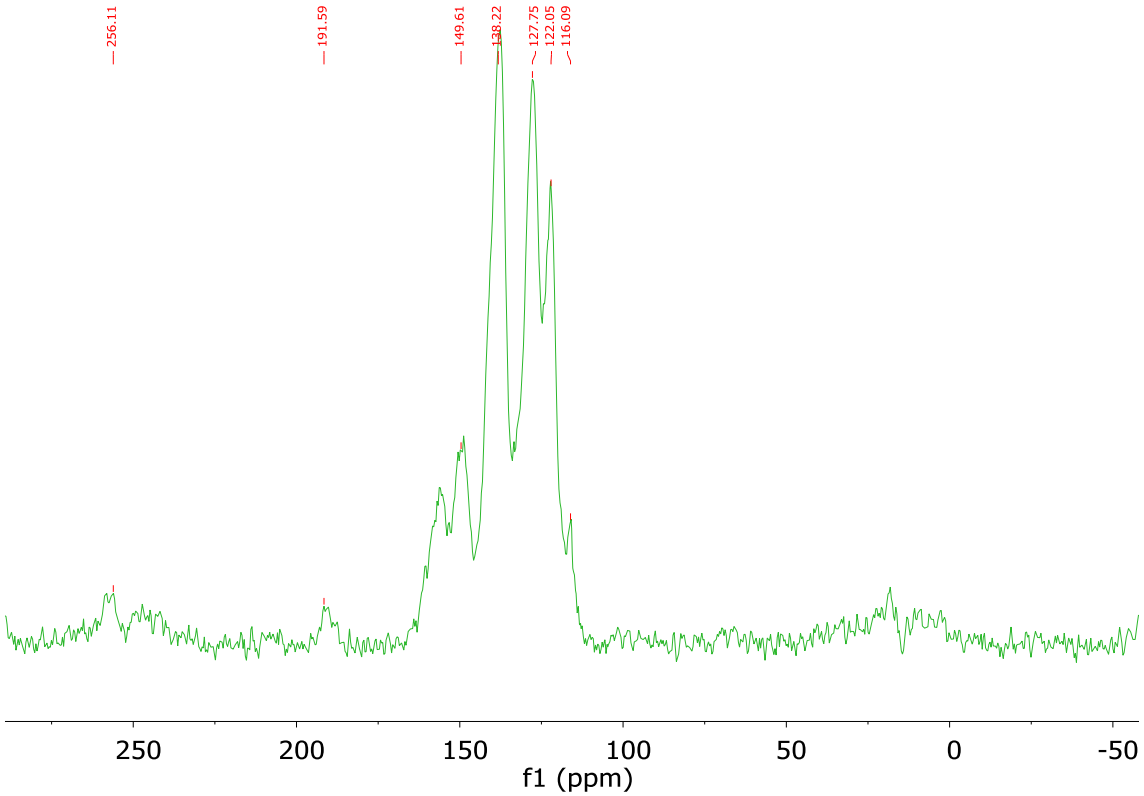

Figure S6. Solid-state ^{13}C CP-MAS NMR spectra of **RT-COF-1Ac**.

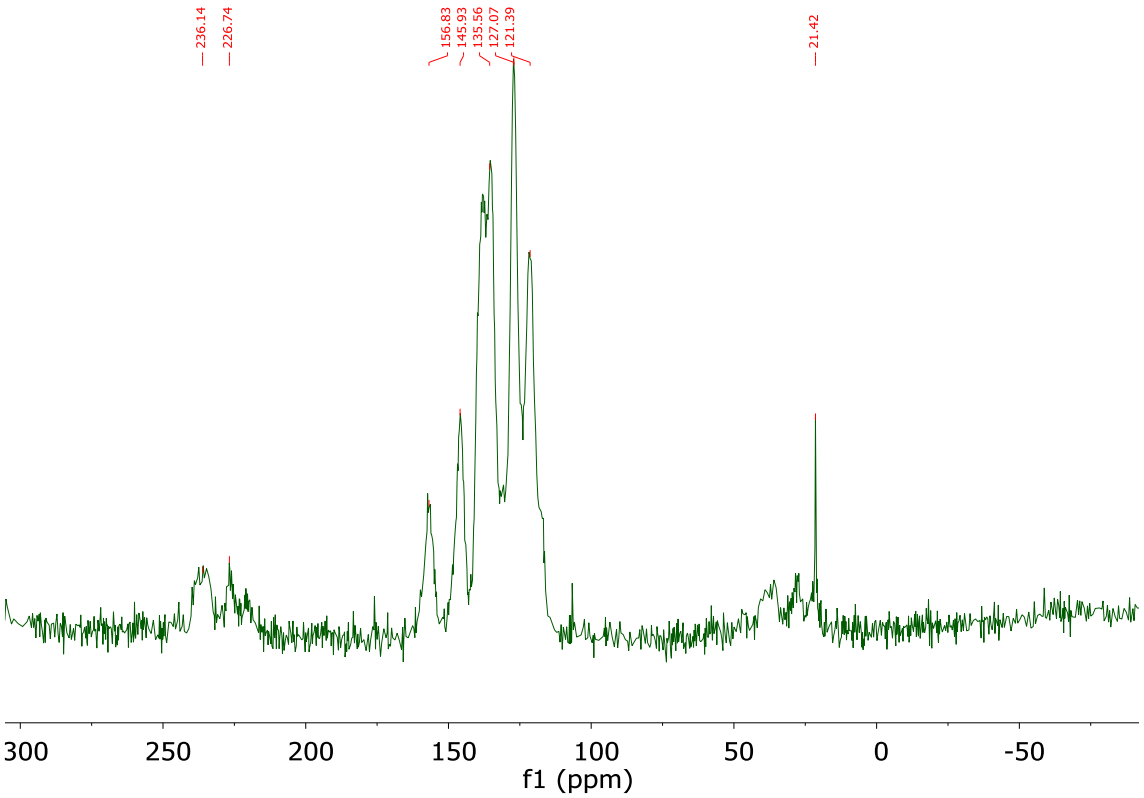

Figure S7. Solid-state ^{13}C CP-MAS NMR spectra of **RT-COF-1AcB**.

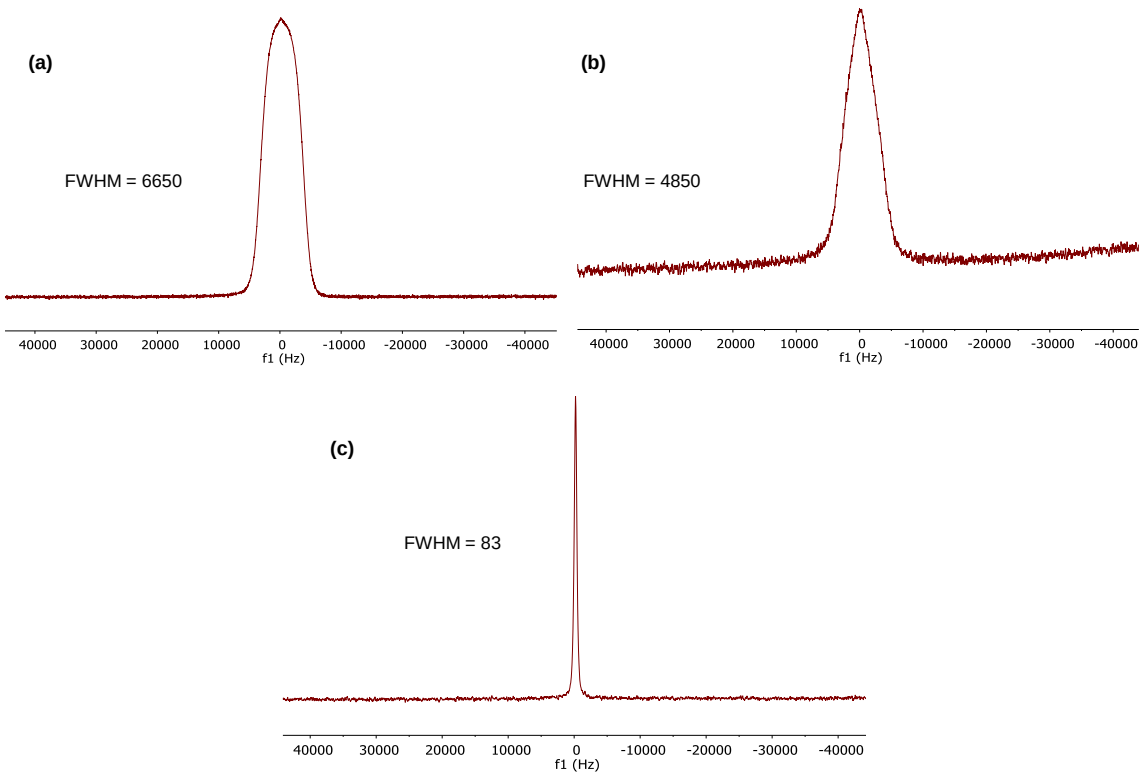

Figure S8. Static ^{7}Li ssNMR spectra at 298 K of (a) pure LiCl at 22 % RH, (b) and (c) of **LiCl@RT-COF-1** at 22 % and 100 % RH, respectively.

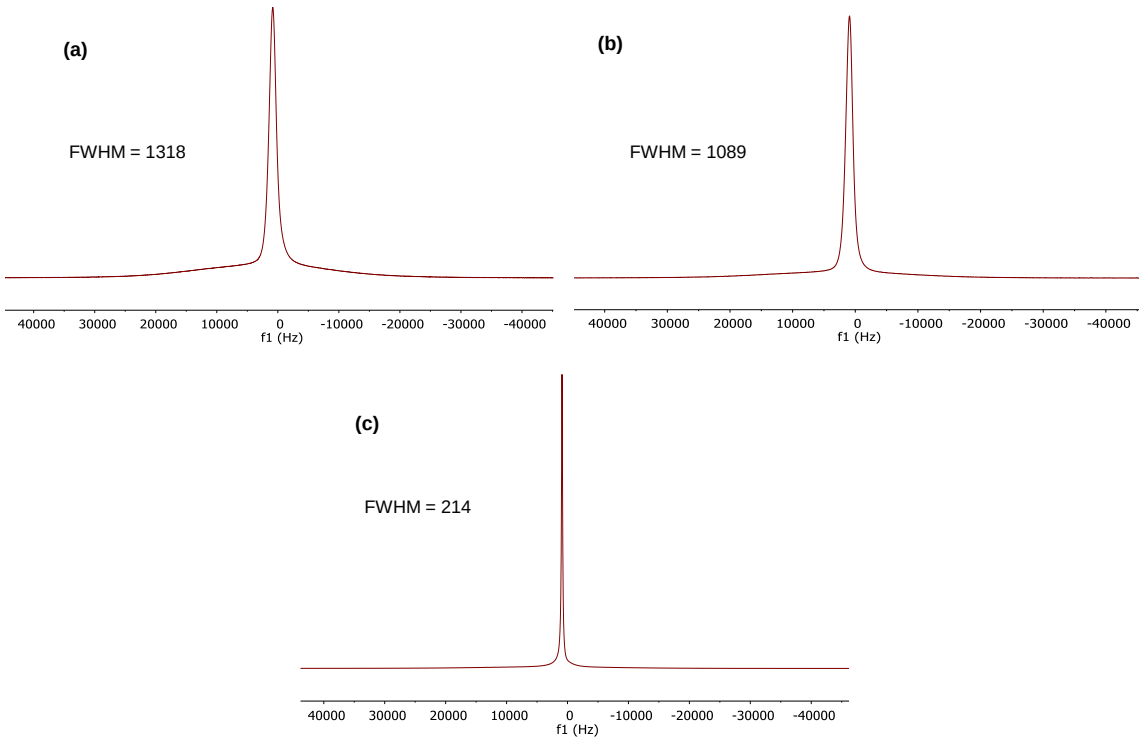

Figure S9. Static ^{1}H ssNMR spectra at 298 K of (a) **RT-COF-1Ac**, (b) **RT-COF-1AcB**, and (c) **LiCl@RT-COF-1** at 100 % RH.

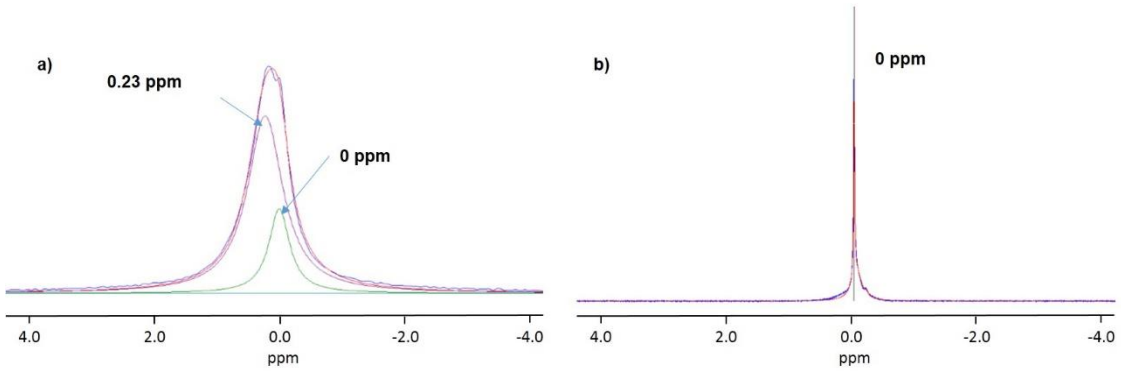

Figure S10. Solid-state ^{7}Li MAS NMR spectra at 298 K of **LiCl@RT-COF-1** (a) at 22 % RH and (b) at 100 % RH.

VII. Thermogravimetric Analysis

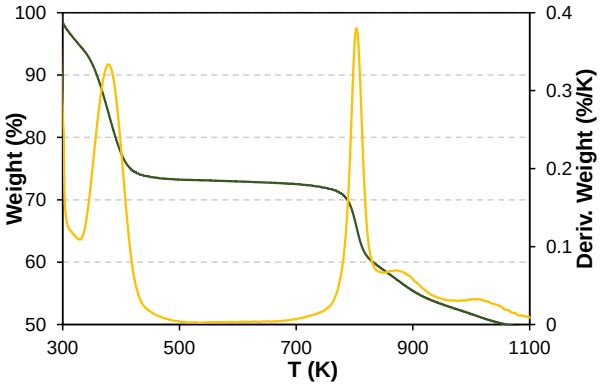

Figure S11. TGA traces and DSC for the species **RT-COF-1AcB**.

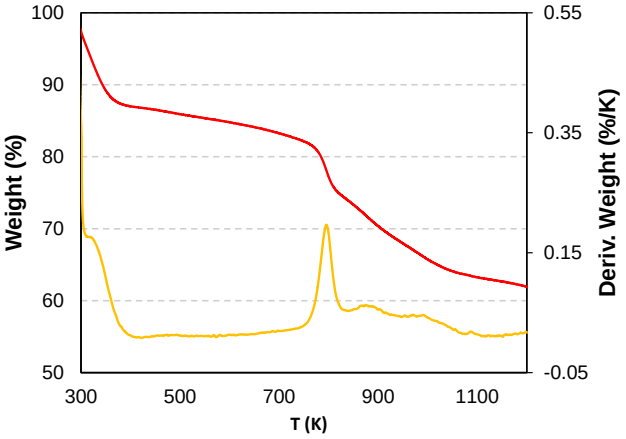

Figure S12. TGA traces and DSC for the species **LiCl@RT-COF-1**.

VIII. N_2 adsorption isotherms

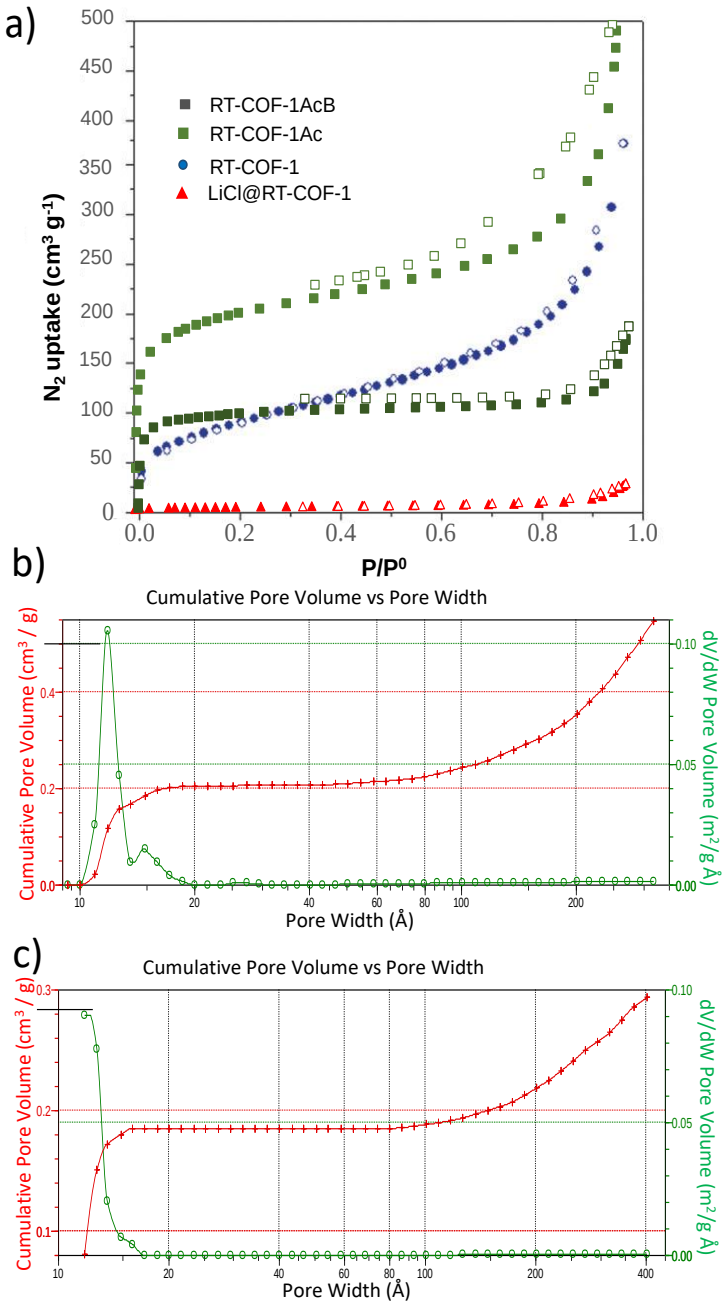

Figure S13. a) Impact of post-synthetic treatment on N_2 adsorption (77 K) for **RT-COF-1**, **RT-COF-1Ac**, **RT-COF-1AcB** and **LiCl@RT-COF-1** materials. Filled and open symbols correspond to adsorption and desorption processes, respectively. b) Pore size distribution for **RT-COF-1Ac**: BET surface of 750 $m^2\ g^{-1}$, micropore volume of 0.2 $cm^3\ g^{-1}$and micropore size of 1.2 nm. c) Pore size distribution for **RT- COF-1AcB**: BET surface of 550 $m^2\ g^{-1}$, micropore volume of 0.19 $cm^3 g^{-1}$ and micropore size of ~1.1 nm.

IX. X-ray photoelectron spectroscopy

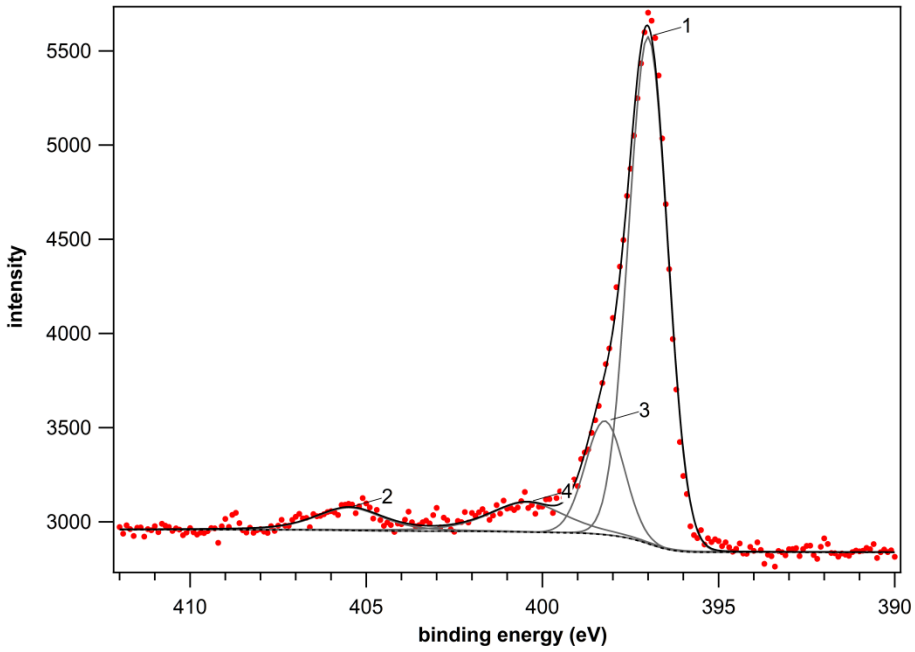

Figure S14. Experimental XPS data and Gaussian fits to the N 1s spectra in **LiCl@RT-COF-1** sample. The line and red points show the fitting curves and experimental data, respectively.

X. Transmission Electron Microscopy

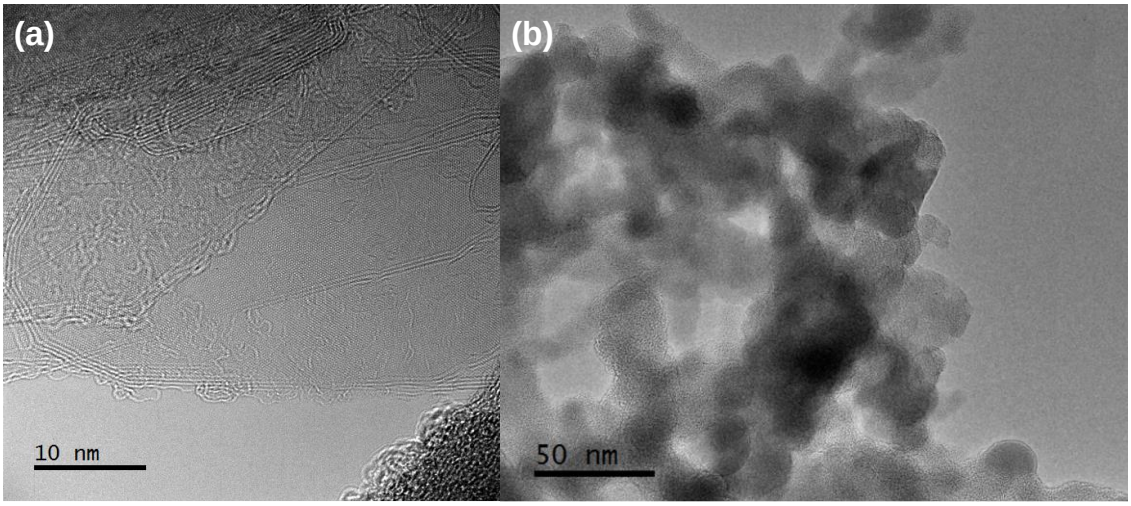

Figure S15. a) HRTEM image of several folded layers. b) Low magnification TEM image showing different layers stacking.

XI. Scanning Electron Microscopy

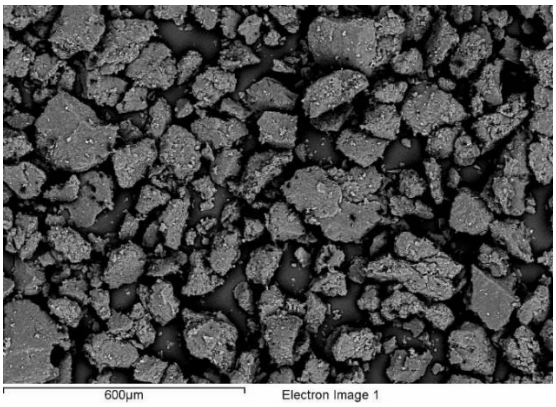

Figure S16. SEM micrograph of **LiCl@RT-COF-1** powder showing irregular particle shape with size around 100 µm**.**

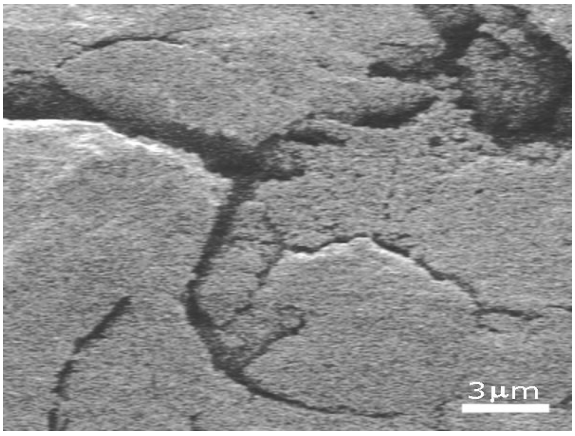

Figure S17. SEM micrograph of a **LiCl@RT-COF-1** pellet showing that the material is poorly compacted and has a great number of fractures.

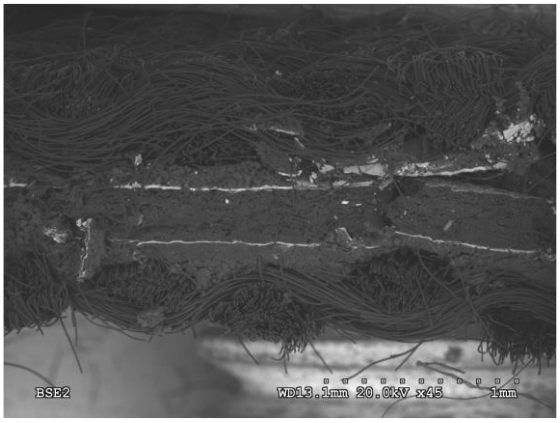

Figure S18. SEM micrograph of MEA cross section of **LiCl@RT-COF-1** film used as solid electrolyte.

XII. Films characterization

Films characterization has been carried out through atomic force microscopy (AFM) and field emission scanning electron microscopy (FESEM).

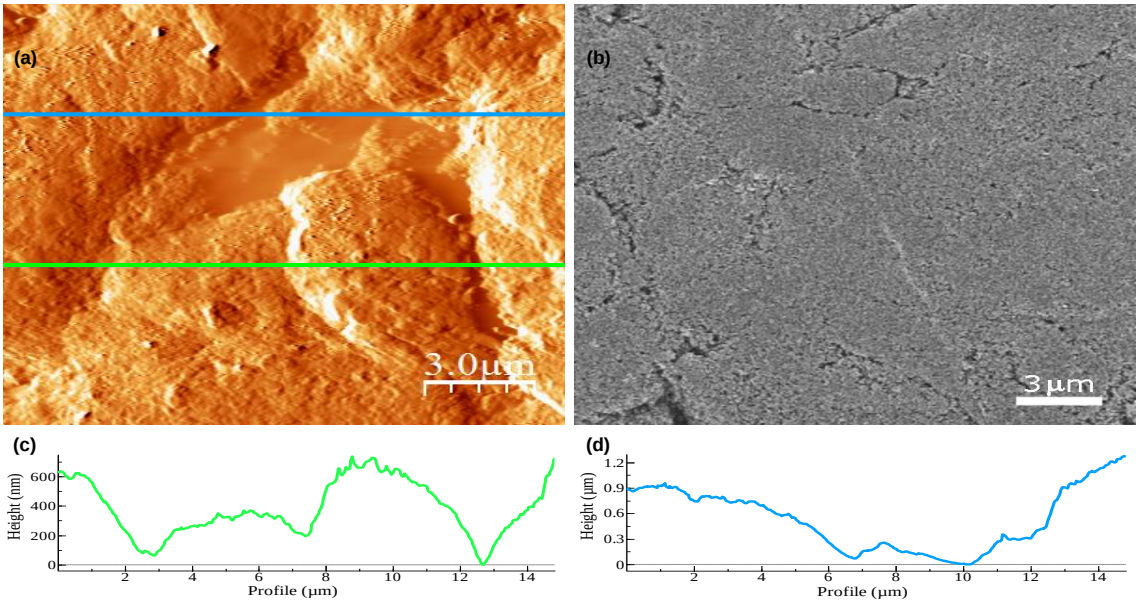

Figure S19. (a) Representative AFM topographic image and (b) FESEM image of **RT-COF-1Ac** film. (c) And (d) profiles were taken along the lines drawn in (a). The surface of this film shows grains of nearly 5 µm in lateral dimensions. While in the majority of the boundaries the grains are tightly packed giving rise to steps 200-400 nm high, in some of the borders there are holes with a diameter of less than 1 µm and that seem to be less than 1 µm deep. By FESEM it can be seen that the distance between holes is around 3 µm.

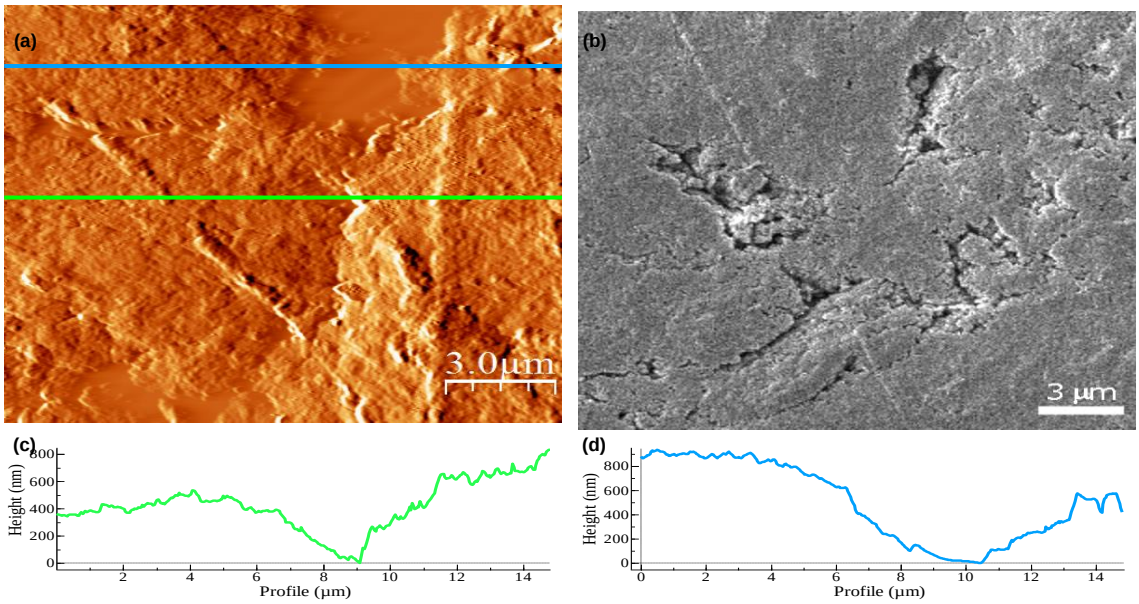

Figure S20. (a) Representative AFM topographic image and (b) FESEM image of **RT-COF-1AcB** film. (c) And (d) profiles were taken along the lines drawn in (a). This film has a similar aspect to **RT-COF-1Ac** film, but in this case the holes reach up to 3 µm in diameter, although they remain quite shallow (depth lower than 1 µm).

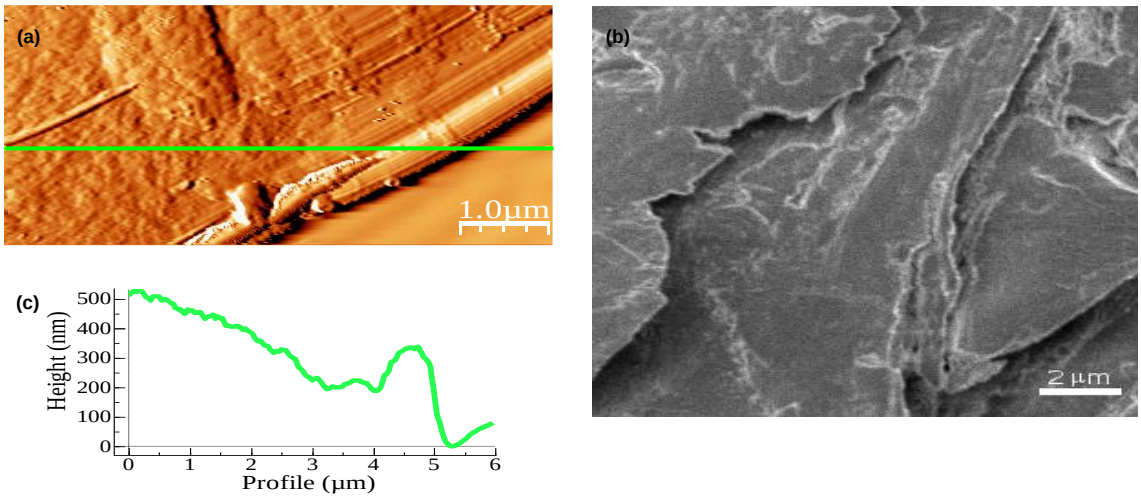

Figure S21. (a) Representative AFM topographic image and (b) FESEM image of **LiCl@RT-COF-1** film. (c) Profile was taken along the line drawn in (a). This film is formed by large pieces of COF. Although each piece is more uniformly compacted than in the previous cases, the boundaries between them are larger and form long and deep cracks 2 µm wide that seem to propagate inside the material.

XIII. Conductivity measurements

EIS data were collected using an Autolab electrochemical system II PGSTAT30 (Ecochemie, The Netherlands) impedance analyzer over the frequency range from 1 Hz to 1 MHz with an AC signal amplitude of 10 mV (rms) around the open circuit potential. All measurements were collected using a two-probe method. AC measurements through path were performed to determine the conductivity parameters at different relative humidity conditions (22 and 100 % RH). The temperature range studied spanned from 298 to 373 K at 22 % RH and 313 K at 100 % RH. The electrical contact between the sample and the symmetric stainless steel disk electrodes, for the through plane measurements, was made by applying a pressure of 350 N cm torque with a conductivity cell configuration SS/COF/SS, where SS refers to stainless steel and COF refers to the pellet of the studied material. Each impedance measurement was repeated three times with different films in order to corroborate the consistency of the conductivity measurements. The conductivity values at different temperatures, σ (S cm^{-1}), and constant humidity (22% RH) were determined from the Nyquist plot by arc extrapolation to the Z´ axis on the high frequency side using the ZView 3.1 (Scribner Association) Software. PXRD patterns of the COF materials were carried out before and after the impedance analyses in order to confirm the integrity of the compound during impedance analysis.

Conductivity measurements at 100 % relative humidity

In order to determine the humidity influence on the conductivity of the COF materials, the samples were exposed to different values of relative humidity (RH) conditions inside a homemade humidity chamber. The 100 % RH value was obtained by bubbling a N_2 flow through ultra-pure water heated at 313 K. The temperature was monitored by using thermocouples placed inside the camera and close to the sample.

Study of the wetting-dewetting reversibility of materials

The reversibility of the **RT-COF-1Ac** and **LiCl@RT-COF-1** materials *versus* moisture was studied by wetting-dewetting cycles (Figure S23). For that, a new film of each material was prepared and placed in the conductivity cell. Then, the conductivity values at 22% RH were measured in the temperature range from 298 to 373 K. At that point, the conductivity cell was cooled to reach 313 K and a new conductivity measurement

was performed before starting the wetting process. After reaching the maximum value of conductivity at 313 K and 100% RH, and concluding with the first cycle of wetting, the material was dried overnight increasing the cell temperature to 373 K. Finally, the second cycle of wetting is carried out following the same procedure described above. All the conductivity values were compared with the ones obtained for another film of the same material in order to ensure the reproducibility of the measurements.

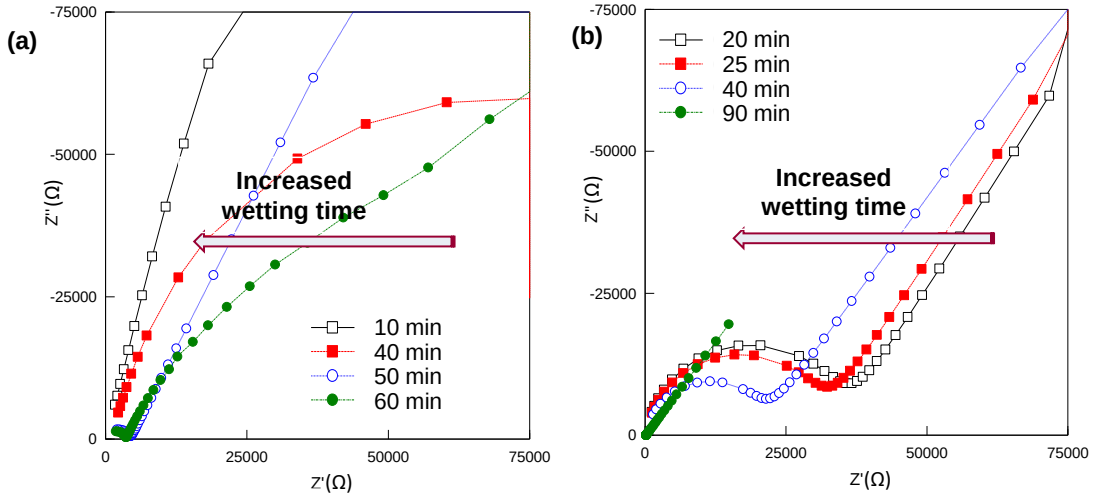

Figure S22. Nyquist plots for (a) **RT-COF-1** and (b) **RT-COF-1Ac** at 100 % RH and 313 K.

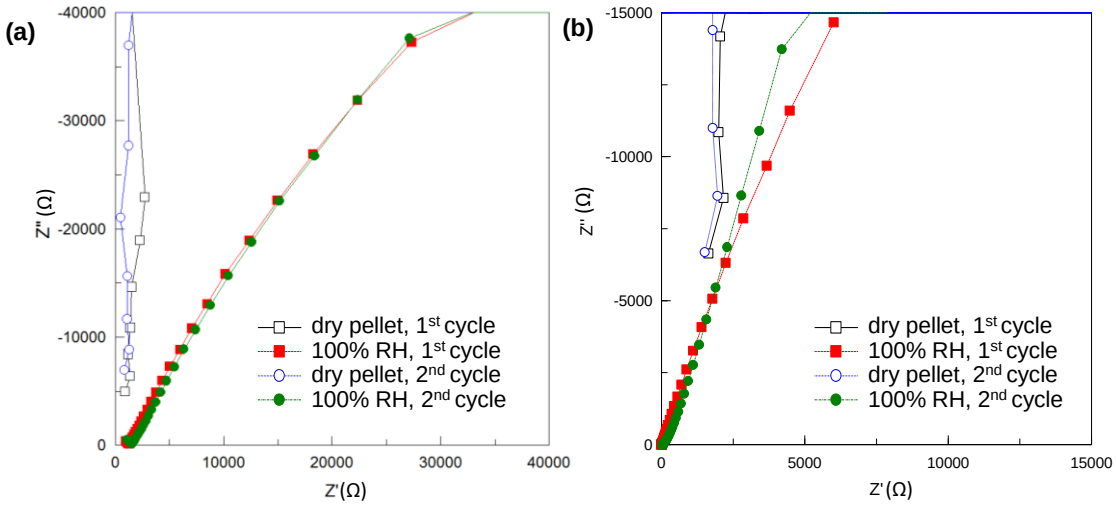

Figure S23. Nyquist plot for the wetting-dewetting cycles of (a) **RT-COF-1Ac** and (b) **LiCl@RT-COF-1** at 313 K.

XIV. Fuel Cell measurements

Membrane-electrode assembly (MEA) fabrication was performed using a standard polymer electrolyte membrane fuel cell (PEMFC) protocol (Figure S24). **RT-COF-1Ac**, **RT-COF-1AcB** and **LiCl@RT-COF-1** films were used as solid electrolyte. Commercial Pt/C catalyst (40 wt.%, Johnson Matthey) was sprayed onto a carbon cloth gas diffusion layer (ELAT GDL-LT 1200W) and used as electrode. The ink was prepared by mixing the catalysts powder with an isopropanol/deionized water solution (2:1 vol.) and a 4 wt.% amount of Nafion® ionomer solution (5 wt. %) on the dry electrode. Pt loading on the electrodes was set to 0.4 mg cm^{-2}. The membrane was then sandwiched between electrodes into the single-cell (Electrochem Inc.) with a final active area of 0.78 cm^2.

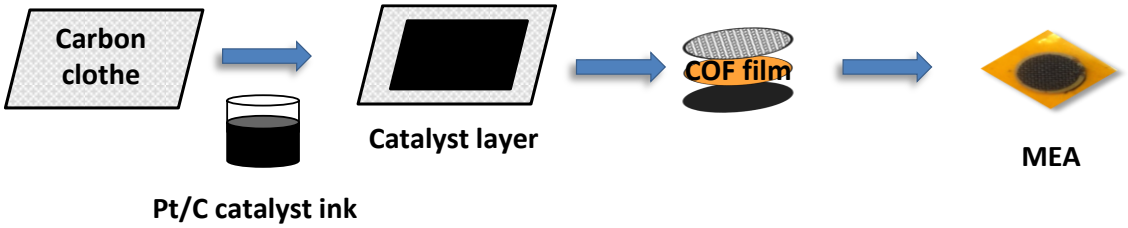

Figure S24. Schematic representation of the MEA preparation using COF film as solid electrolyte.

To study this MEA, we used a test station (FCTS series, Arbin Instruments) controlled with an electrical load system (MITS PRO-FCTS series, Arbin Instruments). The anode and cathode was fed with a flow of 40 mL min^{-1} at atmospheric pressure and 100% of relative humidity (RH) of pure H_2 and O_2 (Air Liquide), respectively. The operating temperature was maintained at 303 or 323 K. The low flow of gas was used in order to prevent the mechanical breakdown of the film.

The electrochemical impedance spectroscopy (EIS) measurements were performed with an Autolab potentiostat with FRA. The measurements were carried out in the frequency range from 10^6 to 10^{-2} Hz with an AC perturbation of 0.01V and open circuit potential (OCP).

A linear sweep voltammetry (LSV) was also measured in the constituted single-cell. The cathode was evaluated as working electrode and the anode as reference and counter electrode. Measurement was performed with and Autolab potentiostat between 0.1 and 0.7 V *vs* OCP at 2 mV s^{-1} scan rate.

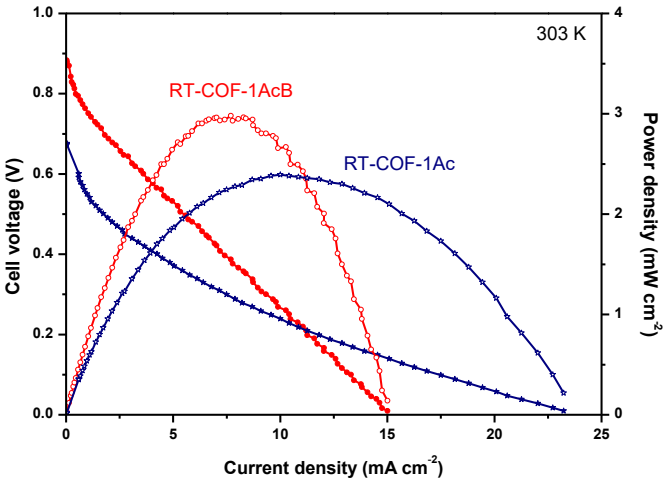

Figure S25. Polarization (filled symbols) and power density (open symbols) curves of **RT-COF-1Ac** and **RT-COF-1AcB** measured at 303 K for a single H_2/O_2 PEMFC.

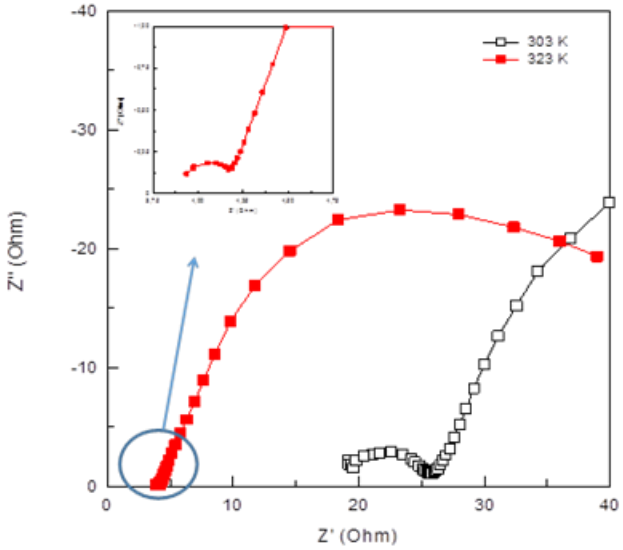

Figure S26. Nyquist diagrams of **H_2(Pt)/RT-COF-1Ac/(Pt)O_2** PEMFC at 303 K (Black open squares) and 323 K (Red open squares). The inset corresponds to a zoomed area showing the characteristic semicircle.

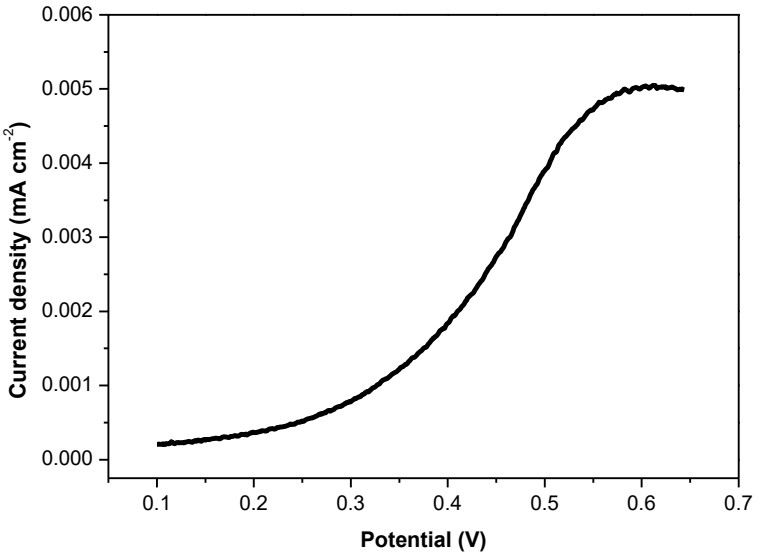

Figure S27. Lineal Sweep Voltamogramm for hydrogen crossover in MEA with **RT-COF-1Ac** film as electrolyte after 6 hours of operation.

XV. References

(1) de la Peña Ruigómez, A.; Rodríguez-San-Miguel, D.; Stylianou, K. C.; Cavallini, M.; Gentili, D.; Liscio, F.; Milita, S.; Roscioni , O. M.; Ruiz-González, M. L.; Carbonell, C.; Maspoch, D.; Mas-Ballesté, R.; Segura, J. L.; Zamora, F. *Chem. Eur. J.* **2015**, *21*, 10666-10670.

(2) Rodriguez-San-Miguel, D.; Abrishamkar, A.; Navarro, J. A. R.; Rodriguez-Trujillo, R.; Amabilino, D. B.; Mas-Balleste, R.; Zamora, F.; Puigmarti-Luis, J. *Chem. Commun.* **2016**, *52*, 9212-9215.

(3) Xu, H.; Gao, J.; Jiang, D. *Nat. Chem.* **2015**, *7*, 905-912.